Letter

Nucleation of Graphene Layers On Magnetic Oxides: CoO(111) and CrO(0001) from Theory and Experiment

John D. Beatty, Tao Cheng, Yuan Cao, Marcus Sky Driver, William A. Goddard, and Jeffry A. Kelber

J. Phys. Chem. Lett., **Just Accepted Manuscript** • DOI: 10.1021/acs.jpclett.6b02325 • Publication Date (Web): 14 Dec 2016

Nucleation of Graphene Layers on Magnetic Oxides: $Co_3O_4(111)$ and $Cr_2O_3(0001)$ from Theory and Experiment

John Beatty, [†,∥] *Tao Cheng,* [‡,∥] *Yuan Cao,* [†] *M. Sky Driver,* [†] *William A. Goddard III** [‡] *and Jeffry A. Kelber** [†]

[†] Department of Chemistry, University of North Texas, 1155 Union Circle, #305070, Denton, TX 76203-5017, U.S.A.

[‡] Materials and Process Simulation Center, Department of Chemistry, California Institute of Technology, Pasadena, California 91125.

Corresponding Author

* Email: wag@wag.caltech.edu; ORCID:0000-0003-0097-5716

*Email: Jeffry.Kelber@unt.edu or kelber@unt.edu

ABSTRACT

We report *directly grown strongly adherent graphene* on $Co_3O_4(111)$ by Carbon molecular beam epitaxy (MBE) at 850 K and DFT findings that the first graphene layer is reconstructed to fit the Co_3O_4 surface, while subsequent layers retain normal graphene structure. This adherence to the Co_3O_4 structure results from partial bonding of half the carbons to top oxygens of the substrate. This structure is validated by X-ray photoelectron spectroscopy and low energy electron diffraction studies, showing layer-by-layer graphene growth with ~ 0.08 electrons/carbon atom transferred to the oxide from the first graphene layer, in agreement with DFT. In contrast, for Cr_2O_3 DFT finds no strong bonding to the surface and C MBE on $Cr_2O_3(0001)$ yields only graphite formation at 700 K, with C desorption above 800 K. Thus strong graphene-to-oxide charge transfer aids nucleation of graphene on incommensurate oxide substrates may have implications for spintronics.

TOC GRAPHICS

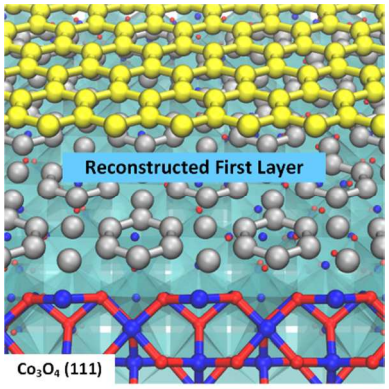

The long spin-diffusion length and high mobility of graphene make it attractive for emerging spintronics applications, [1-2] but the relative inefficiency of spin injection is a significant drawback.[3] Thus, it is of considerable interest to use a magnetic insulator substrate or overlayer to induce spin polarization in graphene by interfacial spin interactions.[4-7] This would make industrially practical and scalable methods of growing graphene directly on such magnetic insulators of great technological and scientific significance. Recently, we used C MBE on $Co_3O_4(111)$ to demonstrated [8-9] several layers of azimuthally oriented graphene. For spintronic device applications growing similar films on $Cr_2O_3(0001)$ would offer several important advantages compared to other oxides because of its magnetoelectric properties [5, 10] and the ability to produce a single magnetic domain via field cooling.[11] However, we find that C MBE on chromia yields only disordered graphite below ~ 800 K and the desorption of C above this temperature. In this paper, we use experiment and DFT to understand the origin of this dramatic difference between growth of graphene on $Co_3O_4(111)$ compared to $Cr_2O_3(0001)$ to provide insight into developing guidelines for obtaining cohesive graphene/oxide films.

Both oxides have similar in-plane O-O distances ~ 2.86 Å,[12-13] that are significantly larger than that of graphene, suggesting the need for some covalent bonding to stabilize the first layer of graphene. Since any covalent bonding between C and O would transfer charge to the more electronegative partner, the O, we speculated that a strongly bound graphene on an oxide should transfer charge **from** the graphene **to** the oxide. This could account for the dramatic difference between these oxides since $Co_3O_4(111)$ is p-type which should be favorable for charge transfer **to** the oxide and hence for covalent bonding to the first layer of C, whereas $Cr_2O_3(0001)$ is n-type under UHV conditions,[14] which might be unfavorable. Thus we speculated that interfacial

charge transfer between graphene and the oxide might play an important role in the quality of the graphene overlayer.

Studies of C MBE on $Co_3O_4(111)$ were carried out in a system equipped for XPS, LEED, and MBE that has been described previously.[15] For studies on $Co_3O_4(111)$, Co(0001) films ~ 25 Å – 30 Å thick were deposited directly on commercially available 1 cm x 1 cm $Al_2O_3(0001)$ substrates by MBE at 700 K, as described previously.[8] Film structure, thickness and cleanliness were analyzed by XPS and LEED. XPS spectra were acquired in constant pass energy mode (22 eV) using unmonochromatized MgKα radiation. Co_3O_4 films 10 Å thick were prepared by direct oxidation of Co(0001) (5 x 10^{-7} Torr O_2, 650 K for 40 min) followed by annealing in UHV to ~ 1000 K.

Studies of C deposition on $Cr_2O_3(0001)$/Co(0001) were carried out in a system described previously,[8] equipped for Auger electron spectroscopy (AES) using a cylindrical mirror analyzer and co-axial electron gun, reverse-view LEED, and the same electron beam evaporation source. AES data were acquired at 3000 eV primary beam energy and collected in the integral mode [N(E) vs. E], then differentiated using the commercially available software. For studies on Cr_2O_3, ~ 1000 Å thick Co(0001) films were prepared by sputter deposition in a separate chamber, followed by sample transfer in ambient and annealing in O_2 and H_2 to remove C and O. Cr_2O_3 films were prepared by evaporative deposition of Cr on Co(0001) in ~ 1 x 10^{-6} Torr O_2 at room temperature, followed by an anneal in 1 x10^{-7} Torr O_2 at 800 K, with film structure and cleanliness verified by LEED and AES.

Indeed, our DFT calculations of graphene on $Co_3O_4(111)$ find partial covalent bonding for the first graphene layer with a transfer of 0.083 electrons/carbon atom on average from the graphene, which is consistent with our experiments. In contrast, DFT calculations on

graphene/Cr_2O_3(0001) find very little binding with no charge transfer,[6] which is consistent with our observation that C MBE on chromia yields only disordered graphite below ~ 800 K with desorption of C above this temperature. There is no experimental evidence of C to chromia charge transfer, in agreement with previous DFT calculations indicating oxide-to-graphene charge transfer.[6]

These results suggest strongly that interfacial charge transfer from C **to** the oxide correlates with graphene nucleation. Hence the surface electronegativity or charge character of the oxide might serve as a useful design feature in selecting the oxide and its surface for the graphene/oxide film

To analyze the graphene oxide interface we carried out DFT calculations using the generalized gradient-corrected Perdew-Burke-Ernzerhof (PBE) functional including the D3BJ empirical correction to include London dispersion (vdW attraction). In order to obtain the correct band gap for the bulk phase calculation, we applied on-site Coulomb repulsion Hubbard U terms. The values of the U terms are taken from the work of Chen et al., which has been shown to provide a quite satisfactory description of the electronic structure of bulk Co_3O_4 with U = 4.4 eV applied to the Co^{2+} state , and U = 6.7 eV applied to the Co^{3+}state.[16] For surface calculations, a single U value (-5.9 eV, a weighted average of the two U values) is used for all Co ions due to difficulty in identifying the oxidation states of the surface Co ions and the inconsistency in calculating surface energy. This single U value has been validated to reproduce the surface energy and relative stabilities of polar Co_3O_4(110) surface. [17] We used Ultrasoft pseudopotentials to describe the O 2s, 2p and Co 3d, 4s valence electrons. We employed Plane wave energy cutoffs of 500 eV to ensure good convergence of the properties. All calculations were performed within the plane-wave pseudopotential scheme as implemented in the Vienna Ab initio Simulation

Package (VASP) 5.3.1. Spin polarization was always included to describe exchange and correlation.

Calculations of bulk Co_3O_4 were performed using the 14-atom primitive unit cell of the spinel *F*d-3m structure. We used a 6×6×6 k-point grid to obtain a well-converged sampling of the Brillouin zone.

Surfaces were modeled using a periodic slab geometry, with consecutive slabs separated by a vacuum layer 15 Å wide. To study the properties of a single A or B termination, we considered symmetric slabs with odd numbers of layers, so that the total dipole moment is zero. Although non-stoichiometric, these models provide useful information in the thick sample limit, when the effect of non-stoichiometry becomes negligible.[18] Structural optimizations were carried out by relaxing all atomic positions until all forces were smaller than 1×10^{-2} eV/A.

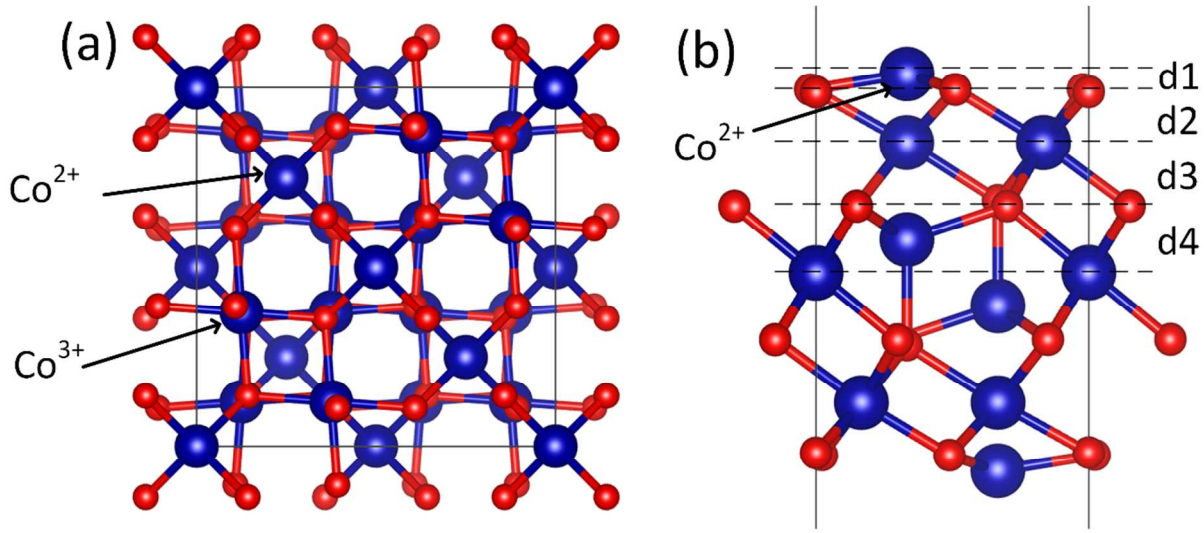

Figure 1. Crystal structure (a) and surface structure (b) of Co_3O_4 optimized using PBE-D3+U DFT, starting from the experimental crystal structure of Co_3O_4 (*F*d-3m). Experimentally, Co_3O_4 is a paramagnetic semiconductor at room temperature. In this spinel structure, Co^{2+} and Co^{3+} are

located at the interstitial tetrahedral (8a) and octahedral (16d) sites, respectively (as labeled in a). Co^{2+} is in a d^7 configuration with three unpaired electrons, and Co^{3+} is in a d^6 configuration with all the d electrons paired. In the bulk calculation, the effective U values used 4.4 and 6.7 eV for Co^{2+} and Co^{3+} from literature.[16] In surface calculations, a single U value (0.59 eV) for all Co ions. [17] The labels in (b) are the distance of Co-O on the surface.

Figure 1 a shows the crystal structure of Co_3O_4 (*F*d-3m). This spinel structure contains one Co^{2+} and two Co^{3+} per formula unit which are located at the interstitial tetrahedral (8a) and octahedral (16d) sites, with 8 tetrahedral and 16 octahedral sites per cubic cell. Co^{2+} is expected to have a d^7 high spin configuration with three unpaired electrons, while Co^{3+} is expected to have a d^6 configuration with all the d electrons spin paired. The PBE-D3+U DFT calculations lead to cell parameters for Co_3O_4 within 1% of the experimental data,[19] as shown in Table 1.

Table 1. Comparison the experimental bulk structure [19] and surface structure [12] with the DFT predicted structures, The distances perpendicular to the surface (d1 to d4) are labeled in Figure 1b. All distances are in Å.

	Bulk	(111) surface			
	cell parameter (a)	d1	d2	d3	d4
PBE+U (Å)	8.113	0.29	0.92	1.04	0.61
Exp (Å)	8.084	0.32	0.95	0.99	0.65

The surface structure predicted by DFT calculations is also consistent with experiment. We considered a symmetric slab as shown in Figure 1b. The first four Co-O distances on the surface were well reproduced by DFT calculation as shown in Table 1. To describe the bonding of graphene to the Co_3O_4 (111) surface, we started with one layer of graphene distorted by 15% to

match the distances of the (111) surface o Co_3O_4 (5.72 × 5.72 $Å^2$) versus graphene (4.92 × 4.92 $Å^2$), which leads to a 26% mismatch in the area. We stretched the graphene to match the Co_3O_4 cell parameters. Therefore, all energies are referenced to the stretched graphene. The optimized structure of one layer graphene on the oxide surface is shown in Figure 2a and 2c. The first contact layer is rugged with the largest distance between rugged graphene of 2.67 Å (as shown in Figure 2 C), much smaller than the interlayer distance in graphite (3.40 Å). This indicates a stronger interaction between graphene and Co_3O_4 than that between graphene and graphene in graphite. Indeed, energy calculations show that the complex is stabilized by 0.193 eV/atom.

$$\Delta E = \frac{E^{Complex} - (E^{graphene} + E^{sur})}{N_C} = -0.193 \ eV/atom \quad (1)$$

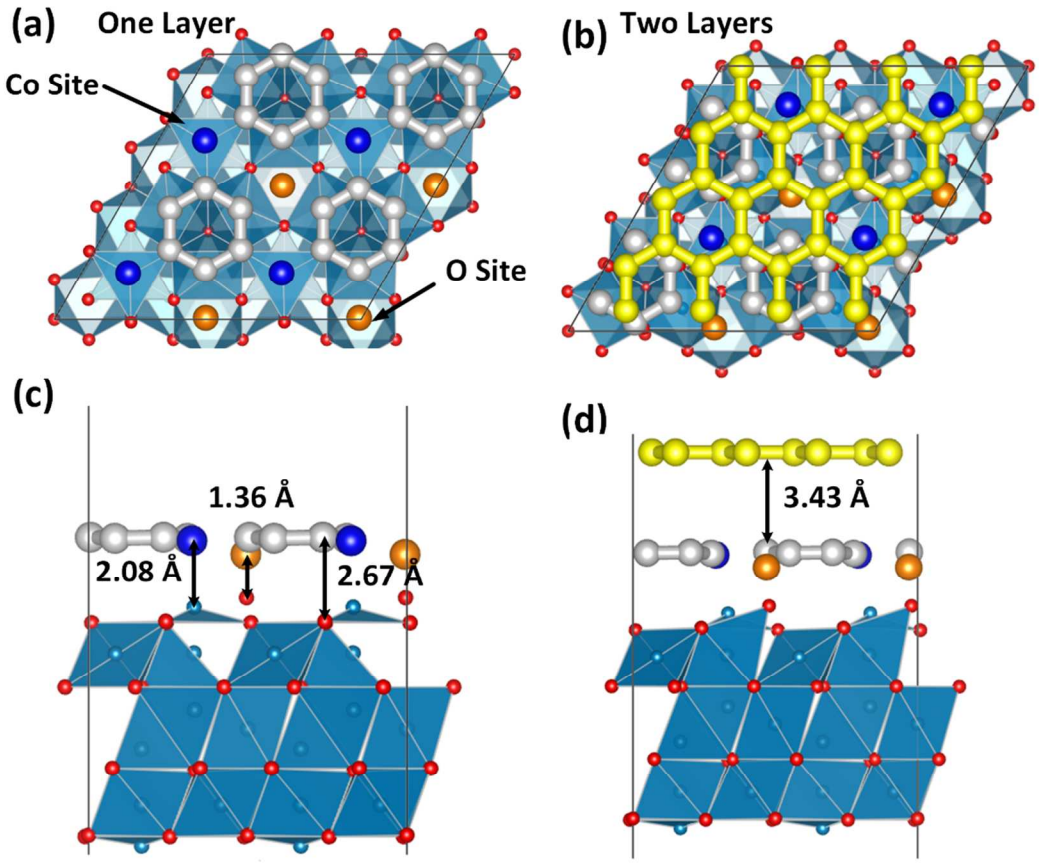

Figure 2. The interface structure of graphene bonded to Co_3O_4 (111) predicted from DFT calculation: (a) and (c) show the top view, and side view of one layer of graphene on Co_3O_4 (b) and (d) show the top view and side view of two layers of graphene on Co_3O_4. The first contact layer of graphene is jagged due to bonding between the C of graphene with the O of the Co_3O_4 surface, while the second layer of graphene is very flat. The colors are Co in blue, O in red, C of the second layer in yellow, C of C6 ring in the first layer in silver, C on Co site in dark blue and C on O site in orange.

The second layer of graphene was flat with mean square displacement less than 0.002 Å. The distance between the first layer and the second layer of graphene is 3.42 Å, very close to the interlayer distance in graphite, which indicates that the interaction should be close to pure graphene. Indeed, we calculate a binding energy per carbon of 0.068 eV between the 1st ML and the stretched 2nd ML, which is 0.015 eV stronger than between stretched graphene or unstretched graphene, 0.053 eV.

The calculations show that the first layer of graphene has a stronger interaction with Co_3O_4, which may be explained by the charge transfer. This -0.193 eV/atom (or -4.44 kcal/atom) energy difference is still within the range of noncovalent interactions, but much stronger than in graphite (0.05 eV/C atom). This stronger interaction may help the nucleation of graphene growth on the Co_3O_4 surface.

Our XPS data (Figure 3) are consistent with the calculations, indicating strong graphene-to-oxide charge transfer. C MBE at 850 K on a 10 Å thick Co_3O_4(111) film on Co(0001) was carried out at intervals, with annealing to 1000 K in UHV after each deposition. Prior to deposition, the Co 2p intensity (Figure 3a, solid trace) indicates Co_3O_4, but upon deposition of a 7.9 Å average thickness C film or ~ 2.4 monolayers (ML) of graphene, the resulting spectrum

(Fig. 3a, open circles) shows a loss of intensity in the binding energy region of ~ 779– 784 eV, corresponding to reduction in the relative intensities of both Co^{+2} and Co^{+3} species.[20] This decrease in intensity corresponds to a decrease in average oxide thickness from 10 Å to 7 Å. Take-off angle-resolved Co 2p spectra (see Supplemental Information, Fig. S1) indicate that this oxide reduction to metal occurs near the Co oxide/Co metal interface. The amount of oxide reduced shows no further change with the formation of additional graphene layers, indicating that the cobalt oxide reduction coincides with the growth of the initial 1-2 graphene monolayers. The Corresponding C 1s spectra (Fig. 3b, solid trace) indicate that the initial C deposition yields a C 1s peak binding energy of 285.2 eV. The Co 2p and C 1s XPS spectra, therefore, indicate that initial deposition of graphene on Co_3O_4(111) results in charge transfer from graphene to the oxide, with partial reduction of the Co oxide to metal. This is in close agreement with the theoretical results. Deposition of additional C yields a gradual shift of the C 1s peak binding energy towards 284.5 eV (Fig. 3b) upon deposition of a total of 6.4 ML graphene. The LEED pattern (Fig. 3b inset), shown for the 6.4 ML film, is maintained throughout the C deposition and is the 6-fold LEED pattern characteristic of graphene. The presence of streaks rather than discrete spots indicates that the graphene sheets are azimuthally aligned. The XPS and LEED data, therefore, indicate that graphene-to-oxide charge transfer is confined to the first 1-2 graphene ML, again in excellent agreement with the calculations.

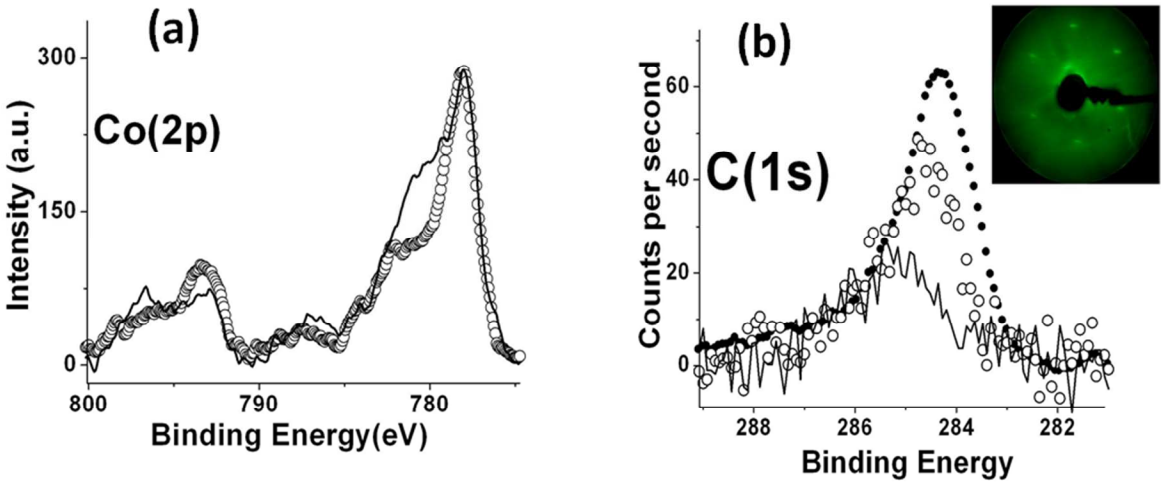

Figure 3 XPS spectra after C MBE on Co_3O_4(111): (a) XPS Co $2p_{3/2}$ spectrum before (solid trace) and after (open circles) 2.4 ML graphene deposition. The spectra have been normalized to equal maximum intensities to illustrate changes in peak shape. (b) Evolution of C 1s XPS spectra upon C deposition at 850 K and annealing to 1000 K after each deposition: (solid trace) 2.4 ML; (open circles) 5.2 ML; (closed circles) 6.4 ML. (Inset) LEED spectrum of 6.4 ML film (150 eV beam energy).

While it is difficult to quantify the amount of charge transfer directly from the XPS data, previously published [8] spectroscopic ellipsometry data show that graphene deposition on Co_3O_4 yields a 0.7 eV blue shift in the graphene $\pi \rightarrow \pi^*$ transition relative graphene on SiO_2 or SiC. model in which the energy shift is due to interfacial dipole approximation. Assuming the sudden approximation,[21] one has:

$$\Delta E = \rho\mu/\varepsilon \quad (2)$$

where ρ and μ are the dipole density and magnitude, and ε is the (out of plane) graphene dielectric constant, taken in the low field limit.[22] The existence of such interfacial dipoles is demonstrated by Raman data showing substrate-induced enhancement of the graphene D peak intensity—the only graphene mode with an out-of-plane vibrational component.[8-9] Assuming ΔE

~ 0.7 eV, equating ρ with the density of C atoms in a single graphene layer, and assuming a dipole charge separation distance of ~ 3 Å yields an estimate of charge transfer of ~ 0.08 electrons/C atom in the initial graphene layer. Given the obvious uncertainties and approximations, including the number of graphene layers involved in the charge transfer, this figure should be regarded as an estimate only, perhaps to within a factor of 2, but it is again closely consistent with the results of the DFT calculations.

We also used C-MBE to deposit a 10.5 Å form of C on Cr_2O_3(0001) at 700 K. This yielded a significant C(KVV) AES feature (Fig. 4a, filled circles) characteristic of sp^2 C,[23] but no observable LEED spectrum. Annealing of the disordered graphitic layer to > 800 K in UHV resulted in apparent desorption of essentially all the C (Fig. 4a, open circles) and a resulting LEED image (Fig. 4b) characteristic of the ordered chromia/Co metal bilayer. C deposition at temperatures > 800 K resulted in no significant C deposition on the chromia surface. The data in Fig. 4 indicate that C MBE on Cr_2O_3(0001)/Co(0001) at < 800 K yields only weak C/oxide interaction, a disordered C layer, with desorption of C from the chromia surface at > 800 K in UHV. This is in stark contrast to C MBE on Co_3O_4(111)/Co(0001),

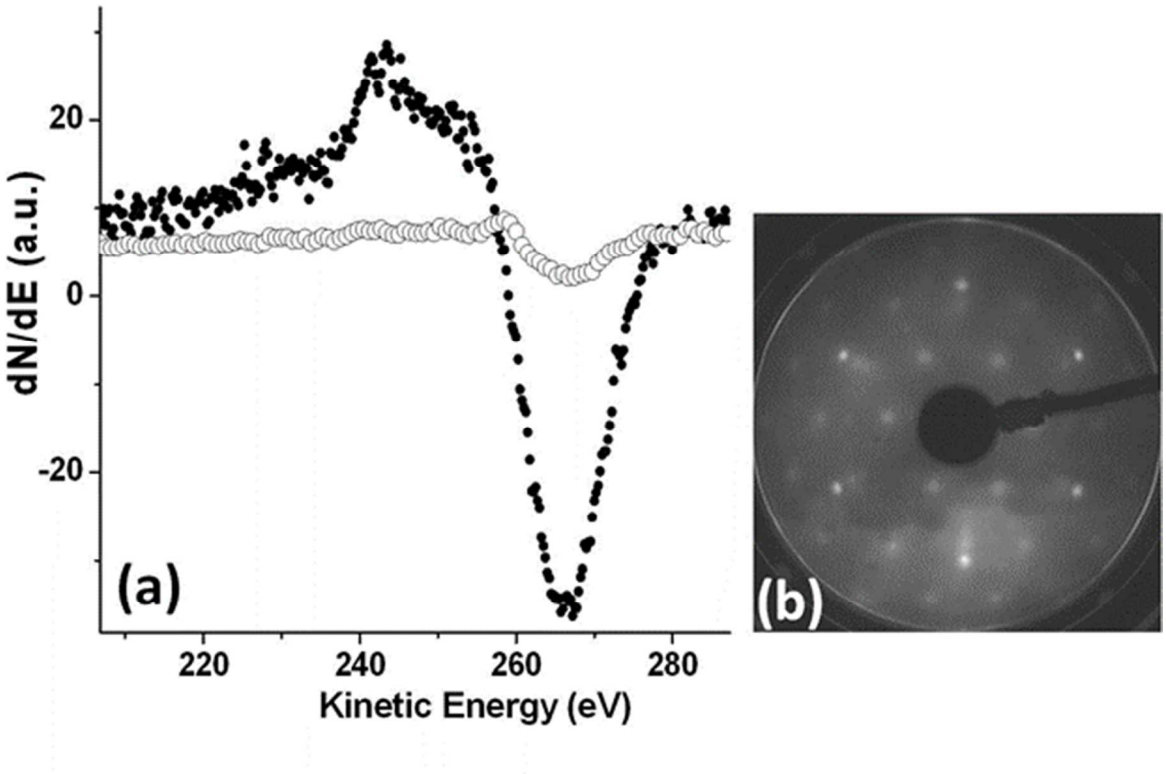

Figure 4. C MBE on Cr_2O_3(0001)/Co(0001): (a) AES C(KVV) feature after C MBE at 700 K (filled circles) and after annealing to 850 K in UHV (open circles); (b) LEED image after C deposition at 700 K and annealing to 850 K in UHV, indicative of a vicinal Cr_2O_3(0001) surface. (LEED beam energy 150 eV).

The weak interaction of MBE C with Cr_2O_3(0001) is in direct contrast with the strong C interaction and graphene formation observed on Co_3O_4(111) under nearly identical conditions. While the possible occurrence of interfacial charge transfers in the C/Cr_2O_3(0001) cannot be inferred from the Auger data, previous DFT calculations on this system[6] indicate that charge transfer would flow from chromia to the graphene overlayer-opposite of what is observed for C/Co_3O_4(111). The differences in charge transfer in the graphene/Co_3O_4 and graphene/Cr_2O_3 systems cannot be ascribed to work function differences since the work functions of both oxides and graphene are all in the range of 4.5 eV – 4.8 eV.[24-26] We attribute differences in behavior for

graphene on the two oxides are to band bending in the oxide at the oxide/C interface. Co_3O_4 is a p-type oxide, while Cr_2O_3 is n-type, at least under UHV conditions.[14] The presence of positive charges in cobalt oxide surface states would enhance charge transfer from C to the oxide, whereas this would not be true for the chromia system.

In summary, theory and experiment indicate that C MBE on Co_3O_4(111) results in graphene nucleation in which the partial bonding of the surface C to the substrate O atoms leads to an average charge transfer of 0.083 electrons/carbon atom from the 1st ML to the oxide. We find that half of the surface C form partial bonds to substrate O with an average charge transfer of +0.138 (see Figure S2) and that this charge transfer is confined to the first graphene layer. In contrast, C MBE on Cr_2O_3(0001) yields only weakly interacting graphite at 700 K, with C desorption above 800 K. This is consistent with previous calculations[6] and simple band-bending arguments indicating chromia-to-graphene charge transfer. **Both theory and experiment therefore strongly suggest that the strong charge transfer from graphene to cobalt oxide is a major factor in the nucleation of graphene on this incommensurate oxide substrate during MBE.** We speculate that such charge transfer is a predictive factor in graphene nucleation on other hexagonal oxide substrates.

AUTHOR INFORMATION

Notes

‖ These authors contributed equally to this work.

The authors declare no competing financial interests.

ACKNOWLEDGMENT

Work at UNT was supported by the NSF under grant no. ECCS-1508991, and in part by C-SPIN, a funded center of STARnet, a Semiconductor Research Corporation (SRC) program sponsored by MARCO and DARPA under task IDs 2381.001 and 2381.006. The research at Caltech was supported by the NSF (DMR-1436985) and DOE (DE-SC0014607)

Supporting Information Available: XPS Co(2p3/2) spectra acquired after C deposition and the distributions of charges on Carbon atoms from Bader Charge Analysis. The Supporting Information is available free of charge on the ACS Publications website at DOI: xxxx.

REFERENCES

(1) Tombros, N.; Jozsa, C.; Popinciuc, M.; Jonkman, H. T.; van Wees, B. J. Electronic Spin Transport and Spin Precession in Single Graphene Layers at Room Temperature. *Nature* **2007,** *448*, 571-574.

(2) Dlubak, B.; Martin, M.-B.; Deranlot, C.; Servet, B.; Xavier, S.; Mattana, R.; Sprinkle, M.; Berger, C.; De Heer, W. A.; Petroff, F., et al. Highly Efficient Spin Transport in Epitaxial Graphene on Sic. *Nat Phys* **2012,** *8*, 557-561.

(3) Dlubak, B.; Seneor, P.; Anane, A.; Barraud, C.; Deranlot, C.; Deneuve, D.; Servet, B.; Mattana, R.; Petroff, F.; Fert, A. Are Al_2O_3 and Mgo Tunnel Barriers Suitable for Spin Injection in Graphene? *Appl. Phys. Lett.* **2010,** *97*, 092502.

(4) Haugen, H.; Huertas-Hernando, D.; Brataas, A. Spin Transport in Proximity-Induced Ferromagnetic Graphene. *Phys. Rev. B: Condens. Matter Mater. Phys.* **2008,** *77*, 115406.

(5) Stuart, S. C.; Gray, B.; Nevola, D.; Su, L.; Sachet, E.; Ulrich, M.; Dougherty, D. B. Magnetoelectric Oxide Films for Spin Manipulation in Graphene. *Physica Status Solidi RRL: Rapid Research Letters* **2016,** *10*, 242-247.

(6) Choudhary, R.; Kumar, P.; Manchanda, P.; David J. Sellmyer, D. J.; Dowben, P. A.; Kashyap, A.; Skomski, R. Interface-Induced Spin Polarization in Graphene on Chromia. *IEEE Magn. Lett.* **2016,** *7*, 7407307.

(7) Kelber, J. A.; Binek, C.; Bowden, P. A.; Belashchenko, K. Magneto-Electric Voltage Controlled Spin Transistors. U.S. Patent 9379232, Aug 21, **2014**.

(8) Mi, Z.; Frank, L. P.; Peter, A. D.; Alex, B.; Mathias, S.; Vanya, D.; Rositza, Y.; Lingmei, K.; Jeffry, A. K. Direct Graphene Growth on Co_3O_4 (111) by Molecular Beam Epitaxy. *J. Phys.: Condens. Matter* **2012,** *24*, 072201.

(9) Yi, W.; Lingmei, K.; Frank, L. P.; Yuan, C.; Bin, D.; Iori, T.; Christian, B.; Peter, A. D.; Jeffry, A. K. Graphene Mediated Domain Formation in Exchange Coupled Graphene/Co_3O_4 (111)/Co(0001) Trilayers. *J. Phys.: Condens. Matter* **2013,** *25*, 472203.

(10) Street, M.; Echtenkamp, W.; Komesu, T.; Cao, S.; Dowben, P. A.; Binek, C. Increasing the Néel Temperature of Magnetoelectric Chromia for Voltage-Controlled Spintronics. *Appl. Phys. Lett.* **2014,** *104*, 222402.

(11) He, X.; Wang, Y.; Wu, N.; Caruso, A. N.; Vescovo, E.; Belashchenko, K. D.; Dowben, P. A.; Binek, C. Robust Isothermal Electric Control of Exchange Bias at Room Temperature. *Nat Mater* **2010,** *9*, 579-585.

(12) Meyer, W.; Biedermann, K.; Gubo, M.; Hammer, L.; Heinz, K. Surface Structure of Polar Co_3O_4 (111) Films Grown Epitaxially on Ir(100)-(1 × 1). *J. Phys.: Condens. Matter* **2008,** *20*, 265011.

(13) Wende, X.; Kan, X.; Qinlin, G.; Wang, E. G. Growth and Electronic Structure of Cu on Cr_2O_3 (0001). *J. Phys.: Condens. Matter* **2003,** *15*, 1155.

(14) Kofstad, P.; Lillerud, K. P. On High Temperature Oxidation of Chromium: Ii . Properties of and the Oxidation Mechanism of Chromium. *J. Electrochem. Soc.* **1980,** *127*, 2410-2419.

(15) John, B.; Yuan, C.; Iori, T.; Driver, M. S.; Peter, A. D.; Jeffry, A. K. Atomic Layer-by-Layer Deposition of H-Bn(0001) on Cobalt: A Building Block for Spintronics and Graphene Electronics. *Mater. Res. Express* **2014,** *1*, 046410.

(16) Chen, J.; Wu, X.; Selloni, A. Electronic Structure and Bonding Properties of Cobalt Oxide in the Spinel Structure. *Phys. Rev. B: Condens. Matter Mater. Phys.* **2011,** *83*, 245204.

(17) Chen, J.; Selloni, A. Electronic States and Magnetic Structure at the Co_3O_4 (110) Surface: A First-Principles Study. *Phys. Rev. B: Condens. Matter Mater. Phys.* **2012,** *85*, 085306.

(18) Chen, H.; Kolpak, A. M.; Ismail-Beigi, S. Electronic and Magnetic Properties of $SrTiO_3/LaAlO_3$ Interfaces from First Principles. *Adv. Mater.* **2010,** *22*, 2881-2899.

(19) Smith, W. L.; Hobson, A. D. The Structure of Cobalt Oxide, Co_3O_4. *Acta Crystallogr., Sect. B* **1973,** *29*, 362-363.

(20) Petitto, S. C.; Langell, M. A. Surface Composition and Structure of Co_3O_4(110) and the Effect of Impurity Segregation. *J. Vac. Sci. Technol., A* **2004,** *22*, 1690-1696.

(21) Foster, K. W.; Saranak, J.; Dowben, P. A. Spectral Sensitivity, Structure and Activation of Eukaryotic Rhodopsins: Activation Spectroscopy of Rhodopsin Analogs in Chlamydomonas. *J. Photochem. Photobiol., B* **1991,** *8*, 385-408.

(22) Santos, E. J. G.; Kaxiras, E. Electric-Field Dependence of the Effective Dielectric Constant in Graphene. *Nano Lett.* **2013,** *13*, 898-902.

(23) Viljoen, P. E.; Roos, W. D.; Swart, H. C.; Holloway, P. H. Carbon Auger Peak Shape Measurements in the Characterization of Reactions on (001) Diamond. *Appl. Surf. Sci.* **1996,** *100*, 612-616.

(24) Yu, T.; Zhu, Y. W.; Xu, X. J.; Shen, Z. X.; Chen, P.; Lim, C. T.; Thong, J. T. L.; Sow, C. H. Controlled Growth and Field-Emission Properties of Cobalt Oxide Nanowalls. *Adv. Mater.* **2005,** *17*, 1595-1599.

(25) Wilde, M.; Beauport, I.; Stuhl, F.; Al-Shamery, K.; Freund, H. J. Adsorption of Potassium on Cr_2O_3(0001) at Ionic and Metallic Coverages and Uv-Laser-Induced Desorption. *Phys. Rev. B: Condens. Matter Mater. Phys.* **1999,** *59*, 13401-13412.

(26) Yu, Y.-J.; Zhao, Y.; Ryu, S.; Brus, L. E.; Kim, K. S.; Kim, P. Tuning the Graphene Work Function by Electric Field Effect. *Nano Lett.* **2009,** *9*, 3430-3434.